INDONESIAN JOURNAL ON GEOSCIENCE
Geological Agency
Ministry of Energy and Mineral Resources

Journal homepage: http://ijog.geologi.esdm.go.id
ISSN 2355-9314, e-ISSN 2355-9306

Geospatial Tool-Based Geomorphological Mapping of The Lower Kulsi Basin, India

Gitika Thakuriah

Faculty of Earth Science, Geography Department, Cotton University, Guwahati-781001

Corresponding author: gitika.thakuria@cottonuniversity.ac.in
Manuscript received: October, 06, 2022; revised: January, 13, 2023;
approved: May, 14, 2023; available online: August, 10, 2023

Abstract - Detailed geomorphological map of a region provides necessary information on landforms to understand the variations of surface and subsurface processes. Geomorphological maps prepared based on a combined geospatial and field-observation approach are preliminary data for precise, prompt, and efficient watershed-level planning. The Kulsi is a significant left-bank tributary of the Brahmaputra. It has potential for agricultural, land, and water resources, but the region needs to catch up due to frequent climatic-geomorphic hazards. Therefore, this article aims to prepare an object-oriented detailed geomorphological map using geospatial tools. High-resolution satellite images and a digital elevation model were used to generate the detailed geomorphological map of the studied area. The resultant map is verified with extensive fieldwork. The investigated basin is characterized by structural and denudation hills, anthropogenetic escarpment; pediment plain, older and young alluvial plain; active and older flood plain; islands and sandbar deposits, and highly sinuous river and natural and artificial surface waterbodies. The research can contribute to local governments' and communities' land and water resource development plans.

Keywords: geomorphology, morphometry, satellite image, Geographic Information System

© IJOG - 2023

How to cite this article:
Thakuriah, G., 2023. Geospatial Tool-Based Geomorphological Mapping of The Lower Kulsi Basin, India. *Indonesian Journal on Geoscience*, 10 (2), p.229-244. DOI: 10.17014/ijog.10.2.229-244

Introduction

Background

Geomorphological mapping means accurately representing terrain configuration and landforms of the earth surface after systematic investigations and interpretation of morphometry, morphogenesis, morphochronology, and morphodynamic feature of landforms. Detailed geomorphological map is a crucial parameter for sustainable land and water resources management, natural hazard assessment and management, urban development, and land use planning. Geomorphological mapping is time-consuming, expensive, and requires extensive field observation processes prepared by well-skilled geomorphologists. They are prepared not only for their research purposes, but pedologists, environmentalists, ecologists, archaeologists, and land planners can use it on a regional scale, such as environmental management (Cooke and Doornkamp, 1990), land use planning (Bocco *et al*., 2001), cultural heritage conservation (Catani *et al*., 2002), military operation (Tate, 2006; Peter, 2011), soil study (Zinck, 2013), archaeological prospecting (Van Lanen *et al.,* 2015), and urban development (Douglas, 2020).

The availability of new tools such as high-resolution satellite images, global positioning

systems, digital terrain models, and GIS has provided a more effective method for the acquisition, storage, and display of geomorphic features quickly. Contemporary techniques can understand surface processes more clearly in geomorphology than the traditional mapping approaches (Reddy, 2018). GPS survey has become widespread among field geomorphologists (Cornelius *et al*., 2006). A high-resolution satellite image provides detailed information on land surface features and a valuable support to the geomorphic fieldwork and interpretation of landscape on a regional scale (Rao, 2002). Multispectral and microwave sensors may detect slight elevation differences, ground irregularities, and land surface properties such as slope and dielectric behaviour of outcropping material, even in cloudy seasons (Smith *et al*., 2011). A digital terrain model is a standard geomorphological mapping tool (Van Asselen and Seijmonsbergen, 2006). The model provides a 3D representation of the investigated area, allowing observation from different vertical scales (Teeuw, 2007; Aringoli *et al*., 2008). Therefore, the geospatial tools are relevant for geomorphological mapping related to specialized landform study. The method has been applied in many world regimes, and has proven effectively in a geomorphic cartography, such as the geomorphological mapping of Peru Chile Trenches (Lemankova, 2009); the coastal sector of Strandzha Mountain in Ahtopol (Prodanov *et al*., 2019), Kalamas River Delta of Epirus, Greece (Chabrol *et al*., 2022), El Bardawil Lake of northern Siami, Egypt (Embabi and Moawad, 2014); tropical karst environment in southern Brazil (Garcia and Grohmann, 2019); Beijing-Tianjin-Hebei area of China (Fan *et al*., 2020); western Ghats Plain of India (Patel and Pati, 2022); Machoi Glacier Valley, NW Himalaya (Pall *et al*., 2019); Rambiara River Basin of western Himalaya (Shah and Lone, 2019); and Malang Regency of East Java, Indonesia (Bachri *et al*., 2021).

Objectives

The present study aims to bring out a geospatial-based object-oriented, detailed geomorphological map of the lower Kulsi River Basin. The geomorphic features of the basins are interpreted and analyzed using some morphometric parameters.

Geographical Settings

Kulsi River is a northward-flowing river system that drains Assam Plain region and joins into Brahmaputra River. The river is known as Khri in Meghalaya, where the tributaries like Um Krisinya River, Um Siri, and Um Ngi confluence at Ukiam. After reaching the alluvial plain of Assam, the river is known as Kulsi River. The Kulsi Basin develops a dendritic pattern of drainage system in the upper catchment area. The basin has a total area of around 1,953 km^2. Geographically, its latitude and longitudinal extension are 25˚31'58.8"N to 26˚75'3.33"N and 91˚E to 91˚48'30"E, showed in Figure 1. The morphology of the upper catchment area of Kulsi River is moderate to steep, and has elevations ranging from 40 m to 1,227 m above mean sea level. The upper catchment is mainly composed of fine texture soil, the parent material is gneiss, and the downstream section of the river is covered mainly by alluvium. The upper catchment area belongs to the age of Proterozoic structure, while the downstream belongs to the age of Meghalaya formed during Barpeta-I, Sorbhog, and Hauli Formations deposition.

The lower Kulsi Basin is in the subtropical monsoon type of climatic zone with highly seasonal rainfall in summer and dry winter. The average annual rainfall was recorded at 1956.67 mm at Boko rain gauge station located in the central part of the basin (Figure 1). More than 78% of the rain occurs only in summer (May to September), causing surface runoff and flood inundation in the lowland, vulnerability for soil erosion, and landslides on the rugged topography and flood inundation in the lowland of catchment area. The lower Kulsi Basin is located in the southwestern fringe of Guwahati City of Assam. The region has full urban expansion and development potential to reduce ever-increasing population pressure on the city.

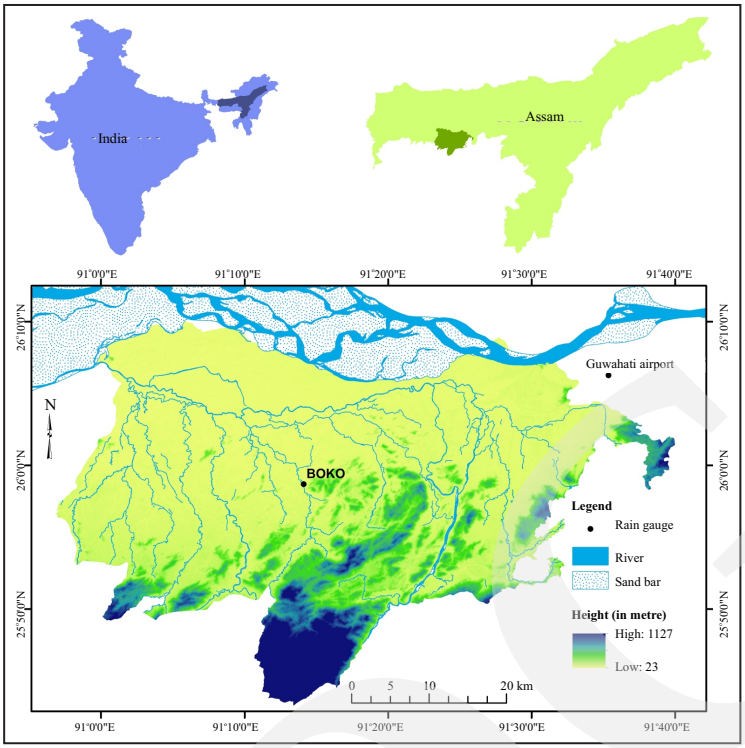

Figure 1. Location map of Kulsi River Basin (Assam part, India).

Materials and Methods

Material

Materials used in this study are shown in Table 1 comprise seven types of data.

Image Interpretation_

Geomorphic Feature Identification

Current physiography was delineated through the digital elevation model generated from a 20 m contour interval of SOI toposheets. The fluvial landforms were identified through a systematic visual interpretation of a high-resolution satellite image, *i.e.* IRS LISS IV with 5m x 5m spatial resolution dated 26th January 2018. The satellite image was projected at the same coordinate system unit, WGS_1984_UTM_Zone_46N. The current physiographic divisions were identified by superimposing the features up to the 1:5000 scale using Arc GIS 10.6 software. The approach

Table 1. Details of Database

Data	Description	Source
Toposheets	Sheet no 78 N/4, 78 N/8, 78 O/1, 78 O/5	SOI, North East Zone Assam Nagaland GDC, Guwahati
	Sheet no 78 O/2, 78 O/6, 78 O/9, 78 O/10, and 78 O/14	SOI, Meghalaya and Arunachal Pradesh GDC, Shillong
Geomorphology	Geomorphic division	Geological Survey of India, www.gsi.gov.in
Geology	Structure, Lineament, Formation, Period	
Soil	Soil map and characteristics	National Bureau of Soil Survey and Land Use Planning, www.nbsslup.icar.gov.in
Hydro-geomorphology	Groundwater prospect and yield	Central Groundwater Board, Northeast Region, Guwahati. www.cgwb.gov.in
Rainfall	Gauge Station: Assam Plain-Guwahati airport, Boko, Goalpara, and Beki Meghalaya Plateau-Shillong, William nagar, and Tikirikila,	Regional Meteorological Centre, Guwahati, India Regional Sericulture Research Station (RSRS), Boko
Satellite image	RISAT 1, MRS 23/09/2014 IRS LISS III, 02/10/2014 IRS LISS IV, 26/01/2018	National Remote Sensing Centre, Hyderabad www.nrsc.gov.in

for preparing the detailed geomorphic map of the studied area involved visual observation, preliminary interpretation using SOI topographical map and Google Earth satellite map provided by land sat/Copernicus 2021, correlation with soil texture and geological structure, and final interpretation after rigorous field check.

Flood Plain Generation

Flood is an annual physio-climatic event in Kulsi Basin. Because of high-intensity rainfall, drainage system, and discharge, physiographic conditions create massive floods, and nearby people are affected annually. The flood plain is delineated from the flood extent of the studied area, which was generated from the satellite image. The flood extent analysis is based on the devastating flood recorded in the last decade, September 2014 (Figure 2). Therefore, satellite data were collected during and after heavy rainfall. During the heavy rainfall, Synthetic Aperture Radar data of RISAT 1, MRS on 23/09/2014 and after one weak of heavy rainfall on 02/10/2014, the optical image of IRS LISS III was collected from National Remote Sensing Centre, Hyderabad (NRSC), (Figure 3).

SAR image

The synthetic aperture radar image is processed using SNAP 8.0.8 and ArcGIS 10.6 software. The required steps for processing SAR images in SNAP tools are subset image, calibration, speckle filtering, and determining a threshold value for image binarization into water and nonwater. Preprocessing calibration and speckle filtering here are done on the subset image. The pixel values in SAR imagery can be related to the radar backscatter of the scene taken. Calibration transforms the pixel values from the digital values recorded by the sensor into backscatter coefficient values. Speckle filtering is just reducing the noise in the image to obtain higher-quality imagery. By determining flooded areas (covered by water) using a histogram of the filtered backscatter coefficient and applying a threshold, the water pixels can be separated from the nonwater pixels. After determining a suitable threshold value, a binary image of water is created (1= true or white) and nonwater (0 = false or black) using the band math of the raster menu. After geometric correction of the binary image, the post processing works are done in ArcGIS 10.6 by Export Image for Viewing in GIS.

Optical image

The flood extent was delineated easily from the optical image through a systematic visual interpretation of satellite image, *i.e.* IRS LISS III, on 2/10/2014 after seven days of heavy rainfall. The flood-inundated areas were digitized after carefully observing the features up to 1:8000

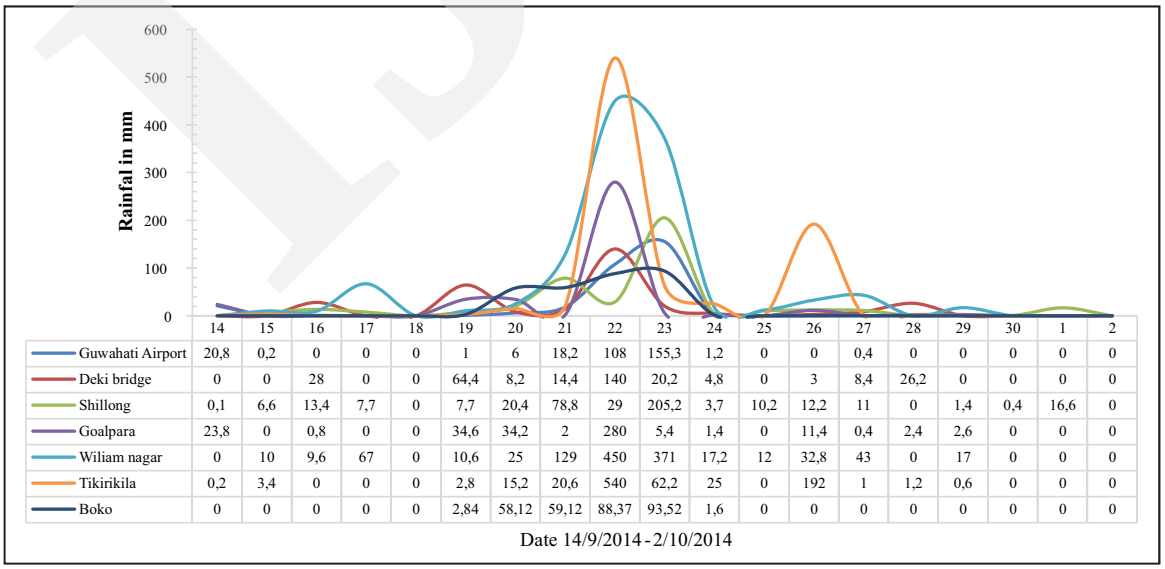

	14	15	16	17	18	19	20	21	22	23	24	25	26	27	28	29	30	1	2
Guwahati Airport	20,8	0,2	0	0	0	1	6	18,2	108	155,3	1,2	0	0	0,4	0	0	0	0	0
Deki bridge	0	0	28	0	0	64,4	8,2	14,4	140	20,2	4,8	0	3	8,4	26,2	0	0	0	0
Shillong	0,1	6,6	13,4	7,7	0	7,7	20,4	78,8	29	205,2	3,7	10,2	12,2	11	0	1,4	0,4	16,6	0
Goalpara	23,8	0	0,8	0	0	34,6	34,2	2	280	5,4	1,4	0	11,4	0,4	2,4	2,6	0	0	0
Wiliam nagar	0	10	9,6	67	0	10,6	25	129	450	371	17,2	12	32,8	43	0	17	0	0	0
Tikirikila	0,2	3,4	0	0	0	2,8	15,2	20,6	540	62,2	25	0	192	1	1,2	0,6	0	0	0
Boko	0	0	0	0	0	2,84	58,12	59,12	88,37	93,52	1,6	0	0	0	0	0	0	0	0

Figure 2. Nineteen-day rainfall record before and after September 2014 flood.

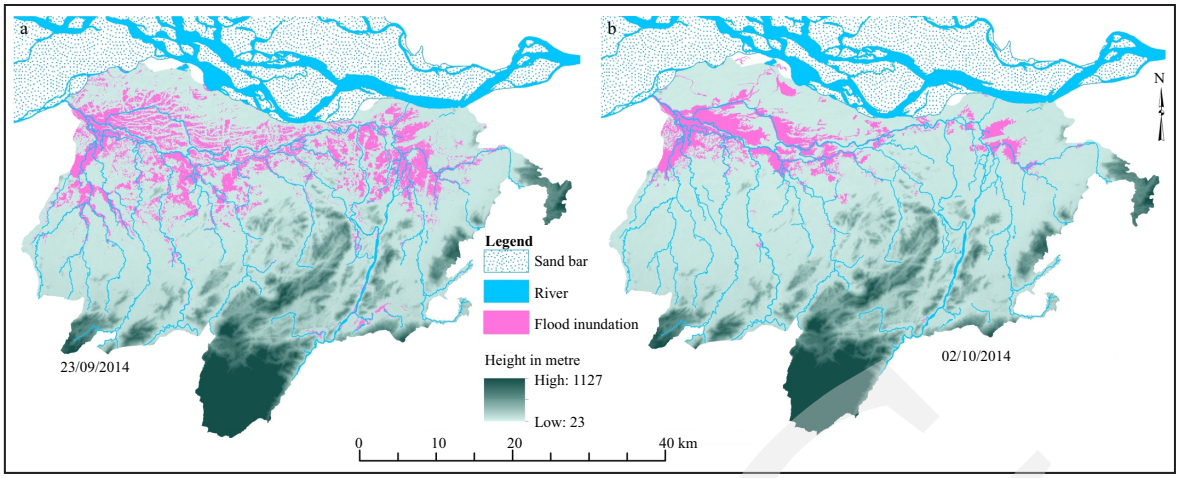

Figure 3. a). Flood inundation: a). During the heavy rainfall, 23/09/2014; b). After ten days of heavy rainfall, 02/10/2014.

scale using Arc GIS 10.6 software. The inundation layer of the flood was overlaid with the current LULC map. The surface water bodies, especially rivers and wetlands from LULC classes were combined with the flood inundation layer to exclude them. The whole approach for preparing an extensive studied area map involved visual observation, preliminary interpretation using SOI topographical map and Google Earth satellite map provided by Landsat/Copernicus 2021, and final interpretation after rigorous field check.

Morphometry of Landform

The quantitative description of surface form is expressed by morphometry, measuring landforms (Gregory and Walling, 1973). It is necessary to express the forms of a drainage basin in the quantitative term to analyze the form-process relationship. The basin morphometric parameters, mainly drainage density, basin relief, basin slope, dissection index, and roughness number, and the channel morphometric parameters like sinuosity index, longitudinal profile and channel gradient, and channel slopes are computed from the Survey of India toposheet at 1:50,000 scale with 20 m contour interval. Table 2 illustrates some morphometric parameters of the basin and channels with detailed mathematical equations.

The drainage density is obtained by dividing the total length of the channel in the basin by the basin total area (Equation 1). The drainage density map of the studied area was prepared using line density arc tools of GIS software. The difference between the maximum elevation point of the catchment and the minimum height in the low-lying area is defined as the basin relief. The DEM is the primary input for the generation of topographic information. DEM for the studied

Table 2. Morphometric Parameter and their Mathematical Expressions

Morphometric Parameter	Equation	Description	Reference	Equation number
Drainage density	$Dd=L/A$	L is the total length of the stream; A is the area of the basin	Horton (1945)	1
Dissection index	$DI=R_R/A_R$	R_R is relative relief, and A_R is an absolute relief.	Dov Nir (1957)	2
Roughness number	$Rn = Dd \times \frac{H}{1000}$	H is basin relief	Patton and Baker (1976)	3
Sinuosity index	$SI = \frac{CL}{MB}$	CL is the length of the channel MB is the length of the meander belt axis	Brice (1982)	4
Stream length gradient index	$SL = \frac{\Delta H \times L}{\Delta L}$	ΔH is the change in reach elevation, L is the total stream length from the source to the reach of interest ΔL is the length of the reach	Hack (1973)	5

area is prepared from the contours of the Survey of India topographic sheet at a 1:50,000 scale with 20 m intervals. A slope map of the basin is prepared with the help of DEM using spatial analysis tools of ArcGIS 10.6 software. The slope measures the steepness or degree of inclination relative to the horizontal plane. The slope is a vertical drop ratio to horizontal distance formed by the earth tectonic or denudation forces. It gives necessary information on the nature of the structure and geodynamic processes at the regional level (Riley, 1999). The nature and magnitude of a terrain can be represented quantitatively through the dissection index and roughness number. The dissection index is a ratio of the maximum relative and absolute relief. The nature of the upland terrain of the lower Kulsi Basin is determined using the dissection index as given by Equation 2 of Dov (1957) and roughness number using Equation 3 given by Patton and Baker (1976).

Channel patterns of a drainage basin are interpreted quantitatively with the help of the sinuosity index (Equation 4). It is a significant morphometric parameter that affects the terrain characteristics of the river course. The relief characteristics of Kulsi River were computed from the longitudinal profile. It is the channel length from the source to the outlet point. It depends on the grade of the slope. The slope of the channel declines gradually depending on the nature of the topography and due to discharge, tectonic activity, geologic structure, sediment transport, flow resistance, width, and depth. The river carries the materials from the source, and starts depositing the materials where the river finds the equilibrium point or the base level. It is the natural law of the river. Displacement along the graded profile would indicate disequilibrium due to tectonic uplift or rock perturbations (Mackin, 1948; Leopold and Maddock, 1953; Whipple and Tucker, 2002; Whittaker *et al.,* 2007). A longitudinal profile measured channel gradient, channel slope, and stream length gradient index. The stream length gradient index of the channel segments is computed using Equation 5, and the index is used for interpreting the morphotectonic evolution of the landform.

Field Survey

A detailed geomorphic map prepared on the basis of the high-resolution satellite image IRS LISS IV, 26/01/2018, as well as GIS techniques are verified successfully with the help of an extensive field survey in the channel and on the basin. The resulting map was compared with the most authenticated map with a 1:50,000 scale of geomorphic division and geology prepared by Geological Survey of India. Whilst a Soil texture map prepared by NBSS, and information on hydro-geology of CGWB, NER, Guwahati. Geomorphic features collected from the field survey are displayed in Figure 4.

Results And Analysis

Geomorphic Division

Geomorphology represents a landform and topographic setting and is crucial in water resource management plans. The detailed geomorphology of the lower Kulsi Basin was prepared based on geomorphic division and geological map prepared by Geological Survey of India, soil texture map prepared by NBSS and LUP, fluvial landforms, channel stability analysis, and flood extent from Spatio-temporal satellite data. The main geomorphic feature in the lower Kulsi watershed is structural and denudation hills, pediment plain, alluvial plain, sand deposits, and surface water (Figure 5). Table 3 illustrates the areal extent of detailed geomorphic division, subdivision, soil texture, hydrogeology, and groundwater prospect. The topographic, drainage, soil, and other condition of each geomorphic feature are discussed below.

Denudation and Structural Hills

The upstream of the studied area comprises moderate and highly dissected structural hills, and the low and moderately dissected denudation hills are low-relief isolated hills in the pediment complex. The relief characteristics of the lower Kulsi Basin are shown in Table 4. Due to continuous erosional processes, the denudational hills have

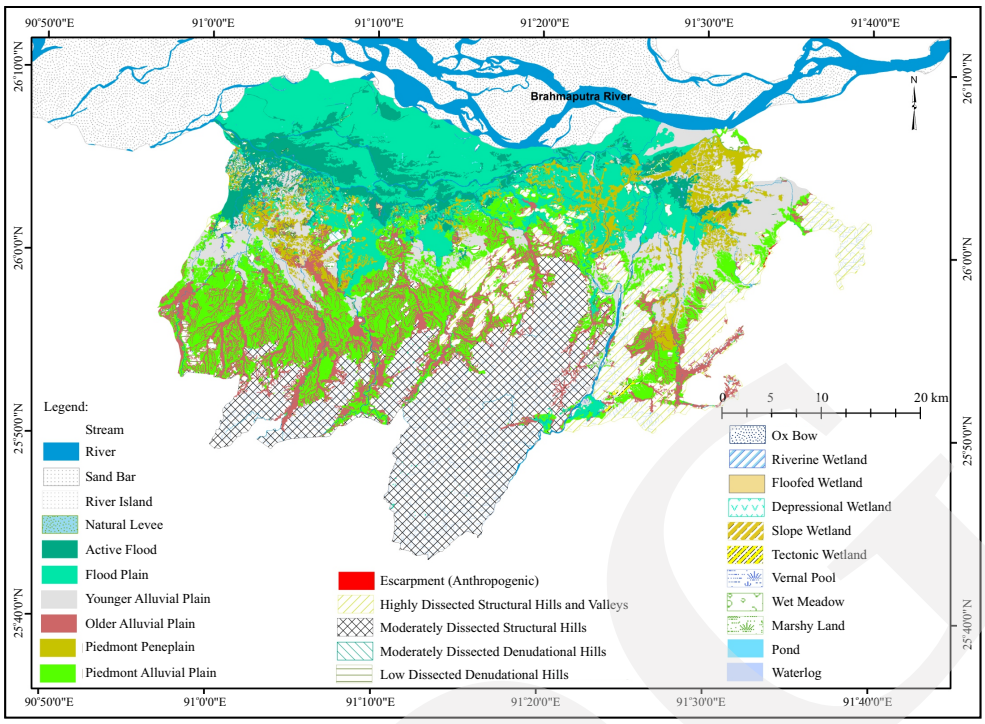

Figure 4. Detailed geomorphologic division map.

a comparatively lower average slope and lower relief landform. The elevation of the denudational hills of the lower Kulsi Basin varies from 41 m - 212 m above mean sea level. The hills are low to moderately dissected by small streams. The drainage density of the region is very low, 0.53 to 1 km/km^2, while the high dissection index of 0.48 and roughness number 7.45 - 9.62 represent highly erosional land surface due to fluvial action. The average estimated rate of soil loss is about 2.02 t ha^{-1}y^{-1}. The southern hill features are controlled by the underlying geological structure of amphibolite, dolerite, and grey and pink porphyritic granite. The elevation of the structural hills varies from 48-1127 m above mean sea level. It is a moderate to a highly dissected hill by numerous streams where the dissection index is found at 0.49 - 0.53, and the high drainage density varies from 1.62 to 2.68 km/km^2, with the average slope of 14.62 degrees, depicting the surface runoff of the rugged hilltop, and are affected by soil erosion. Anthropogenic processes interrupt or break the general topographic continuity of the land surface and produce a relatively steep slope-0.31 km^2 area covered by the anthropogenic escarpment.

Piedmont Plain

The pediment plain is another crucial geomorphic basin unit with a moderate slope sustaining natural vegetation and grassland at the base of the moderately and highly dissected parts of structural Garo Hills. The piedmont plains are subdivided into two geomorphic units: The piedmont alluvial plain and the piedmont peneplain. Piedmont alluvial plains are the deposited landforms created at the foot of Garo Hills by Kulsi and its numerous tributaries. *Piedmont peneplain* is the gentle undulation low featureless plain produced by fluvial erosion. The elevation of the piedmont plan area varies from 36 to 85 m above mean sea level. The landform supports the natural vegetation of Tectona Grandis (Teak) and Shorea Robusta (Sal) species with extensive grassland. The drainage density of the region varies from 0.58 to 1.10 km/km^2 (Table 5).

Alluvial Plain

The low-lying area of The Kulsi Basin is an alluvial plain. The geomorphic subunits of the plain are the younger alluvial plain, older alluvial plain, active flood plain, and older flood plain.

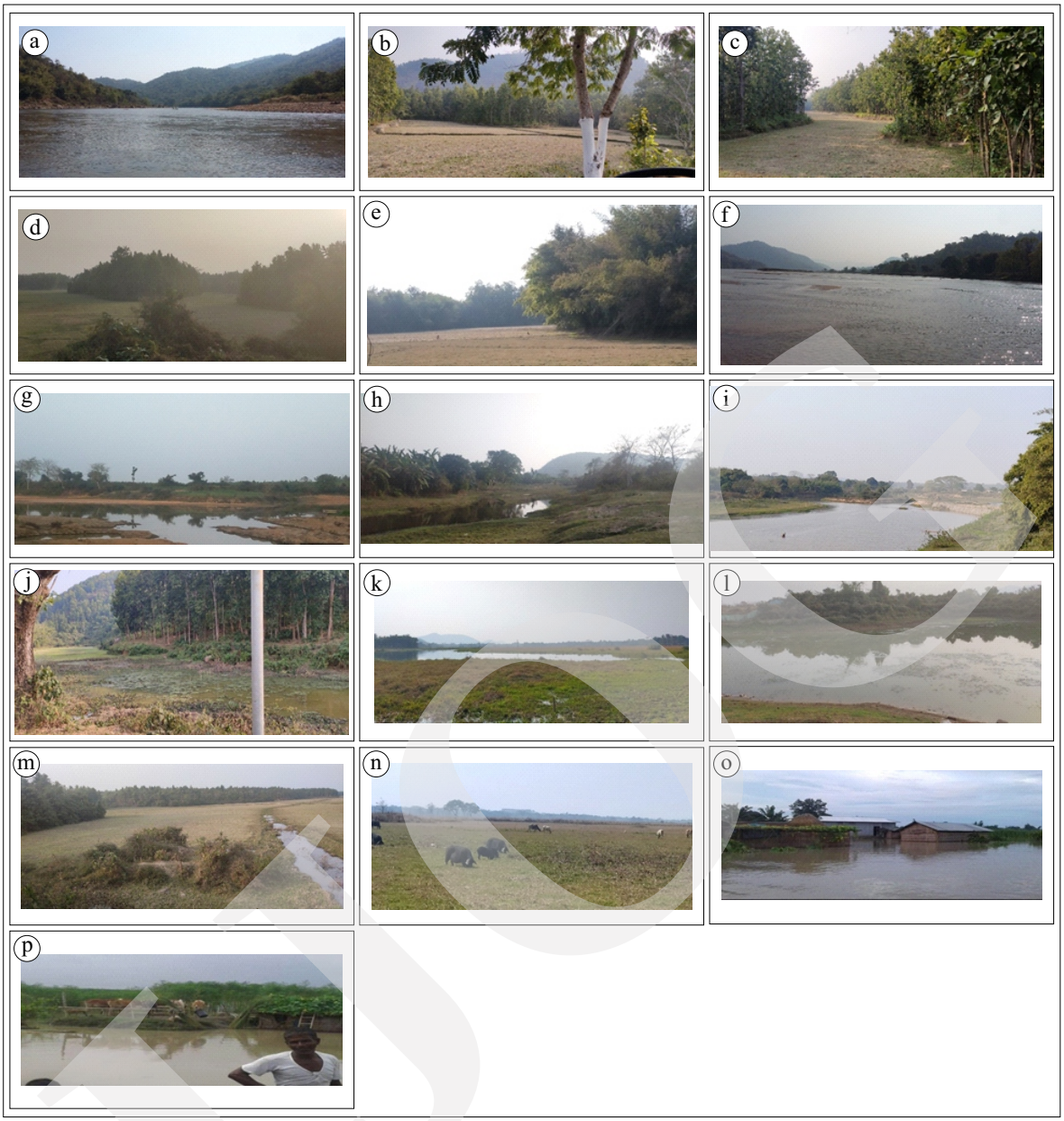

Figure 5. Photographs of: a). Highly dissected structural Garo Hills and Kulsi River at Ukium; b). Overview of hill, piedmont alluvial plain in Kulsi Basin; c). Older alluvial plain in between Sal Forest dominated the piedmont alluvial plain; d). Sal Forest dominated piedmont peneplain complex with older alluvial plain; e). Bamboo-dominated peneplain feature with paddy field on the young alluvial plain; f). Sand bar formation in the bed of Kulsi River near Ukiam; g). Anabranch of Kulsi River near Nalbari Forest Village; h). Formation of river island near Balijori Village by anabranch channel of Kulsi River; i). River Island in Singra River, a tributary of Kulsi River; j). Wetland at the foothills of Gobardhan Hill; k). Gabong slope wetland at the foothills of Kulsi Hill; l). Depressed wetland in Dhanubhanga Reserve Forest; m). Wet meadows in Deosila Reserve Forest; n). Grazing land surrounding the Dora wetland; o). Flood Inundation in Sontali Village (2020); p). Flood impacts on domestic animals, Sontoli Village (2020).

The structure of older alluvium is oxidized to feebly oxidized sand, silt, and clay and highly oxidized, dark brown to red-brown in loamy sand. The composition of the younger alluvium is feebly oxidized sand, silt, and clay and white to greyish-coloured sand, silt, pebble, and clay. The slope gradient of Kulsi River from Ukium (80m) to Nagarbera (35 m) abruptly falls about 46 cm/km. Table 5 shows the relief and drainage characteristics of the alluvial plain of the studied area.

Flood is a significant problem in the studied area, identified as active flood areas, chronically

Table 3. Areal Extent of the Large-scale Geomorphological Map of Lower Kulsi River Basin

Geomorphic division	Landform unit	Areal extent (km²)	Soil texture	Hydrogeology	Groundwater prospect
Hill	Highly dissected structural hills	172.166	Fine clay	Groundwater is restricted to 50 m depth in weathered residues, joints, and fractures having secondary porosity. Thickness in the weathered zone 5-15m.	Low yield prospect up to 5 m3/hr. Dug wells are feasible in weathered zones. Boreholes at fractured zone at selected points
	Moderately dissected structural hills	415.931			
	Moderately dissected denudational hills	4.951			
	Low dissected denudational hills	4.439			
	Escarpment (Anthropogenic)	0.316			
Piedmont Plain	Piedmont alluvial plain	296.580	Fine	Moderately thick but discontinuous confine & unconfined aquifers, a thickness of 10-50m within 50-100m depth.	Suitable for shallow tube well with a yield of 10-20 m3/hr. Deep tubewell up to 100 m depth, yielding 30- 50 m3/hr. Dug well feasible at foothills
	Piedmont peneplain	117.652	Fine, Coarse & Fine loam		
Alluvial Plain	Older Alluvial Plain	160.952	Fine clay & Fine loam		
	Young Alluvial Plain	171.71	Coarse Silt	Relatively thick and regionally extensive confine & unconfined aquifers. Aquifer thickness, 30-70m within 150-300m depth.	Large yield prospect Suitable for shallow tube wells with 30-50m3/hr. Deep tube wells of 150-200 m depth yield 50-150 m3/hr.
	Flood Plain	335.667	Coarse Silt, Fine		
	Active Food Plain	129.194	Coarse Silt		
Surface water	River	38.053	-		-
	Wetland	21.830			
	Marshes	22.76			
Sand deposits	Sandbars	25.700	Coarse Silt	Relatively thick and regionally extensive confine & unconfined aquifers. Aquifer thickness, 30-70m within 150-300m depth.	Large yield prospect Suitable for shallow tube wells with 30-50m3/hr. Deep tube wells of 150- 200 m depth yield 50-150 m3/hr.
	River Islands	30.167			
	Natural levee	0.642			
Total area		1956.490			

Table 4. Landform Units of Hills and their Relief and Drainage Characteristics

Landform units	Areal extent (km²)	Height (m)		Relative relief	Drainage density (km/km²)	Average Slope (Degree)	Dissection index	Roughness number
		Min.	Max.					
Highly dissected structural hills	172.16	42	563	521	1.62	14.51	0.53	9.65
Moderately dissected structural hills	415.93	48	1127	1079	2.68	14.62	0.49	9.86
Moderately dissected denudational hills	4.95	41	190	149	0.99	14.27	0.48	9.62
Low dissected denudational hills	4.44	41	212	171	0.53	11.62	0.47	7.45

Table 5. Landform Units of Pediment Plain and their Relief and Drainage Characteristics

Landform units	Areal extent (km²)	Height (m)		Relative relief (m)	Drainage density (km/km²)
		Min.	Max.		
Piedmont alluvial plain	296.580	38	85	47	1.10
Piedmont peneplain	117.652	36	85	49	0.58

flooded areas, and occasionally flooded areas (Figure 5). Flood occurrences are a natural annual event of the alluvial plain. The area represents a highly vulnerable Kulsi River flood plain, devastated almost annually by floods. These areas are dense populations, and it is observed that the intensity of floods is increasing with time and with a more significant loss.

Table 6. Landform Units of Alluvial Plain and their Relief and Drainage Characteristics

Landform units	Areal extent (km^2)	Height (m)		Relative relief (m)	Drainage density(km/km^2)
		Min.	Max.		
Older Alluvial Plain	160.952	36	422	386	1.26
Young Alluvial Plain	171.71	34	126	92	0.74
Flood Plain	335.667	27	113	86	0.48
Active Food Plain	129.194	28	102	74	0.74

Surface Water

River

Kulsi River is located on the northern front of Shillong Plateau. It originates from the Meghalaya Plateau at 1,700 m above mean sea level in Meghalaya, known as the Khri River. After reaching the alluvial plain, the tributaries, namely Um Krisinya, Um Siri, and Um Ngi, confluence with the Khri River at an altitude of 80 m above mean sea level near Ukiam of Assam. The river is known as Kulsi River. It flows towards the north and drains in the plain region of Assam into Brahmaputra River. Um Krisinya, Um Siri, Um Ngi, Boko, Singra, Singua, and Deosila are left-bank tributaries of Kulsi River. Batha and Umshru are two important tributaries on the right bank. Kulsi and its tributary and anabranches occupy about 38.05 km^2 geographical area. It develops a dendritic pattern of the drainage system in the upper catchment area. As the per stream order method of Strahler, the Kulsi is a ninth-order drainage system. In the lower Kulsi River Basin, 1910 stream segments are delineated in the first order (Table 7). The debris slopes are moderate to severely eroded with finer alluvial soil high acceleration.

The sinuosity index of Kulsi River between Balijori and Brahmaputra confluence near Nagarbera, about 71 km channel reach, was found at 1.20 and 1.24 in the year 1972 and 2018, respectively. It shows that the downstream of Kulsi River is highly sinuous. From Ukium to Balijora, about 22 km, the sinuosity index wasrecognized to be 1.10 in 1972 and 1.05 in 2018. Here low sinuosity index specifies solid structural control and flows over Kulsi Fault line from an approximately straight channel.

Relief Characteristics of Kulsi River

Slope declines gradually depending on the nature of the topography and due to discharge, tectonic activity, geologic structure, sediment transport, flow resistance, width, and depth. In Meghalaya, the river origins at an altitude of 1,700 m near Nonglyer (known as Khri River), the tributaries like Um Krisinya River, Um Siri, and Um Ngi confluence with Khiri River at Ukium. After reaching the alluvial plain of Assam, the river is known as Kulsi River. It runs up to 198.83 km at the outlet point. Figure 6 shows that the Knickpoints about 15.98 km and 53.71 km downstream from Nonglyer are presumably due to the Guwahati Fault passing along Kulsi River course (Yin *et al*., 2010).

On the other hand, the third knick point about 10 km upstream of Ukiam corresponds with the lithological boundary between a Banded Gneissic Complex of Shillong Plateau and the alluvial Assam plain associated with high stream length gradient indices upstream, indicating the tectonic activity in faster erosion (Imsong *et al*., 2018). Table 8 illustrates the slope gradient and stream length gradient index of Kulsi River from Ukium (80 m) to Nagarbera (35 m), abruptly falling about 41 cm/km and 0.02, respectively. The Kukurmara site, about 33.66 km downstream from Ukium reach, has a slope gradient of about 0.98 m/km, indicating that the upstream highly eroded materials are deposited in the downstream and lower course.

Wetlands

Wetlands cover about 51.89 km^2 area of the lower Kulsi River Basin. Based on geomorphic settings, the wetlands of Kulsi River basin are classified as riverine, slope, depressional, vernal pool, marshes, and pond (Table 7).

Riverine wetlands occur in the low-lying flood plains, water blocked in paleochannels, and riparian pathways associated with stream channels. Flooded and oxbow are examples of

Table 7. Landform Units of Surface Water

Landform units	Areal extent (km²)	Classification of geomorphic unit	Number
River	38.053	Mainstream	Kulsi
		Tributary	9
		Anabranch	2
		Streams order	Number of segments
		First	1910
		Second	547
		Third	117
		Forth	34
		Fifth	14
		Sixth	11
		Seventh	4
		Eighth	3
		Ninth	1
Wetland	51.895	Riverine	492
		Oxbow lake	10
		Flooded	119
		Slope	247
		Depressional	348
		Tectonic	6
		Vernal pool	66
		Marshes	803
		Wet meadows	28
		Waterlog	8
		Pond	232

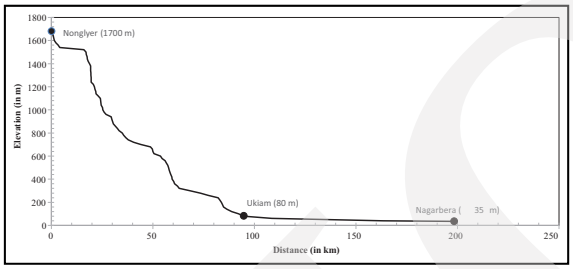

Figure 6. Longitudinal profile of Kulsi River shows major Knickpoints and a high stream gradient in the upper course.

riverine wetlands. Flooded wetlands are formed by overbank flow or subsurface hydraulic connections between the stream channel and wetlands (NRCS, 2008). Oxbow lakes are crescent-shaped riverine water bodies and abandoned meander loops of a channel. It is formed as the river cuts through the meander neck to shorten its course and block off sediment deposits.

Slope wetlands commonly lie on sloping land where groundwater is discharged to the land surface (NRCS, 2008). They are usually incapable of depressional storage, because they necessarily lack closed contours. Slope wetlands can occur in nearly flat landscapes if groundwater discharge is a dominant source of the wetland surface. Slope wetlands lose water primarily by saturation subsurface and surface flows and evapotranspiration.

Depressional wetlands develop in topographic depressions after precipitation, groundwater discharge, and interflow and overland flow from the surrounding uplands toward the centre of the depression (NRCS, 2008). Depressional wetlands may have any combination of inlets and outlets or lack them entirely (NMED, 2012). Tectonic wetlands due to by the tectonic movement-Chandubi wetland of Kulsi watershed formed as the tectonic submergence of forest during earthquake in 1897.

Vernal pools are present as small topographic depressions and isolated wet areas within upland forests with poor drainage, where runoff from rain

Table 8. Relief Characteristics of Kulsi River Computed from Longitudinal Profile

Name	Elevation (in m)	Stream length (in km)	Channel gradient (m/km)	Stream length gradient index
Nonglyer	1700	0	-	-
Ukiam	80	101.11	16.02	3.185
Kukurmara	47	33.66	0.98	0.019
Chamaria	42	38.74	0.12	0.002
Nagarbera	35	25.30	1.38	0.005

collects in spring (Thomson and Sorenson, 2005). They are flooded temporarily for a short time after heavy rainfall every year. Most of the wetlands on the piedmont alluvial plain with dense vegetation covering Kulsi watershed are categorized in the vernal pool.

Marshes are characterized by standing water and emergent vegetation (ANR) such as water hyacinth (*Eichhornia crassipes*), lotus (*Nelumbo nucifera*), water lillies (*Nymphaeaceae*), water caltrop (*Trapa natans*), and water spinach (*Ipomoea Oquatica*). The plants that grow in marshes vary depending on the water depth and the duration of flooding. Wet meadows and marshes of 8.99 km^2 wide are also identified in the lower Kulsi Basin. It is a type of wetland with water-saturated soil supporting grass growth. They are found in the riparian area and land between marshes and upland.

Ponds are natural or artificial shallow and small inland standing water bodies. Two hundred thirty-two smaller natural and artificial ponds are identified in the lower Kulsi River Basin.

Sand Deposits

The Kulsi and its tributaries deposited numerous coarse sand bars along the bank and bed of channels due to decreased stream velocity when they enter gentle sloping foothills. Three hundred ninety-eight sand bars were found in the lower Kulsi Basin covering 25.7 km^2 in 2018. Small river islands are formed by anabranches along the unstable banks and return to the mainstream further downstream. Twenty-one small and large river islands were formed, covering a 30.167 km^2 area in the Brahmaputra and its tributary, Kulsi. It has three river islands by an anabranch channel process near Balijora, Ghormara, and Karidal Villages. The formation of natural levee is another essential characteristic of the Kulsi and its tributaries in the alluvial plain. It is a long, broad natural embankment of sand and coarse silt, built by streams on a flood plain and along both sides of its channel, especially when water overflowing the normal bank is forced to deposit the coarsest part of its load.

Discussion

The field-based geomorphological mapping is time-consuming, cost-intensive, qualitative, and difficult to reproduce (Meij *et al*., 2022). The development of satellite imagery, GPS, and GIS modelling techniques has opened up new opportunities for applied geomorphological surveying and mapping. The combined geospatial tools and field observation-based techniques create an accurate and precise geomorphological map. The past works of literature show that the rapid geomorphic regionalization of the Beijing-Tianjin-Hebei area of China was achieved based on digital terrain analysis through the development of remote sensing and GIS (Zhang *et al*., 2020); field and geospatial-based geomorphological map of Kalamas Delta contains lithology and hydrogeology (Chabrol *et al*., 2022); the geomorphic features of El Bardawil Lake of northern Sinai in Egypt was presented using digital image processing techniques (Embabi *et al*., 2014), the large scale geomorphological map with 1:10,000 scale was created based on digital elevation model for karst environment in southern Brazil (Garcia and Grohmann, 2019). The remote sensing and GIS-based regional geomorphological map can be utilized for land evaluation and land use planning (Bocco *et al*., 2001). The Kulsi Basin is located in the undulating topography with highly seasonal rainfall in summer and dry winter. Below 1% of the total rainfall occurs only in the winter (December to February) causing issues with water shortage, groundwater recharge and discharge in the basin. More than three-fourth of the rain occurs only in summer, leading to surface runoff and flood inundation in the lowland, vulnerability for soil erosion, and landslides on the rugged topography in the catchment. Therefore, the Kulsi Basin of north-eastern India needs large-scale object-oriented landform information for watershed management.

In this research, the geomorphic map of the basin was prepared using high-resolution satellite data (5.8 m) for the first time with reasonable accuracy of the feature observation and 20 m contour DEM for calculating the topographic

factor. The geomorphic features were digitized after carefully observing the features up to the 1:5000 scale using Arc GIS 10.6 software. The correctness of the landform features derived from satellite images was assessed using the point-by-point method to show similarities and differences between the output and geomorphic division of the geological survey of India map layer. The overall accuracy was 0.95, indicating almost perfect strength of agreement between the output feature and ground truth data. The proposed large-scale geomorphic map prepared based on remote sensing, and GIS techniques offers input to land and water resource management of the lower Kulsi Basin. The proposed map would help the decision-makers, urban planners, and local government as an input database to achieve sustainable development and reduce meteor-geomorphic hazards of the basin.

Conclusions

Detailed geomorphological maps act as an essential input in land and water resource management, urban planning and development, hazard risk reduction by demarcating hazard zoning, potential groundwater assessment, and another environmental research. The detailed geomorphological map of Kulsi Basin was performed based on the combined geospatial tools using high-resolution satellite data in Arc GIS 10.8 software and field observation. The resultant geomorphological map of the studied area was further compared with most authenticated governmental datasets, records, and maps. About 30 % of the studied area comprises moderate to highly dissected structural hills, low and moderately dissected denudation hills, and low relief isolated hills in the pediment complex. The lowland includes the piedmont plain and the alluvial plain. The alluvial plains are categorized into the younger alluvial plain, older alluvial plain, active flood plain, and older flood plain with a channel gradient of 0.46 m/km. Temporary sand deposits, river islands, and natural levees are micro- geomorphic features of Kulsi River plain. A detailed geomorphological map can be applied as a preliminary input for watershed management, land and water resource action plans, water harvesting site delineation, potential groundwater zonation, flood and landslide hazard risk management, optimum land use planning, and urban expansion and development of Kulsi Basin. Therefore, the research will contribute to developing the country local governments and communities if the large-scale geomorphic map is used for the land and water resource development plan.

Acknowlwdgement

The author would like to thank the Science and Engineering Research Board (SERB) for its financial support on this project. Special thanks to the scientists of the Regional Sericulture Research Station (RSRS), Boko, for providing rainfall and other meteorological data. The author is thankful to wonderful field assistants, research scholars, and all who indirectly contribute in making this research successful.

References

ANR (Agency of Natural Resources), Wetland Type, Wetland Department of Environmental Conservation, www.dec.vermont.gov.

Aringoli, D., Calista, M., Gentili, B., Pambianchi, G., and Sciarra, N., 2008. Geomorphological features and 3D modeling of Montelparo mass movement (Central Italy). *Engeenering Geology*, 99 (1-2), p.70-84.

Bachri, S., Shrestha, R.P., Yulianto, F., Sumarmi, S., Utomo, K.S.B., and Aldianto, Y.E., 2021. Mapping Landform and Landslide Susceptibility Using Remote Sensing, GIS, and Field Observation in the Southern Cross Road, Malang Regency, East Java, Indonesia. *Geosciences,* 11 (4). DOI: 10.3390/geosciences11010004.

Bocco, G., Mendoza, M., and Velazquez, A., 2001. Remote sensing and GIS-based regional

geomorphological mapping-a tool for land use planning in developing countries. *Geomorphology*, 39, p.211-219.

Brice, J.C., 1982. Stream channel stability assessment. Report FHW A/RD-82/021, US Department of Transportation Federal Highway Administration, Washington, DC 42.

Catani, F., Fanti, R., and Moretti, S., 2002. Geomorphologic risk assessment for cultural heritage conservation. *In*: Allison, R.J. (ed.), *Applied Geomorphology*. John Wiley & Sons, Chichester, p.303-316.

Chabrol, A., Gonnet, A., Fouache, E., Pavlopoulos, K., and Lecoeur, C., 2022. Geomorphology of the Kalamas river delta (Epirus, Greece). *Journal of Maps*, 18 (2), p.276-287. DOI: 10.1080/17445647.2022.2046654.

Cooke, R.U. and Doornkamp, J.C., 1990. *Geomorphology in Environmental Management. A New Introduction. Second ed.* Oxford University Press, Oxford, 410pp.

Cornelius, S.C., Sear, D.A., Carver, S.J., and Heywood, D.I., 2006. GPS, GIS, and geomorphological fieldwork, *Earth Surface Processes and Landforms,* 19 (9), p.777-787.

Douglas, I., 2020. Urban geomorphology. In: Douglas, I., Anderson, P.M.L., Goode, D., Houck, M.C., Maddox, D., Nagendra, H., and Yok, T.P. (eds) *The Routledge Handbook of Urban Ecology*. Abingdon: Routledge.

Dov, N., 1957. The ratio of relative and absolute altitude of Mt. Camel., *Geographical Reviews* 47, p.564- 569.

Dramis, F., Guida, D., and Cestari, A., 2011. Nature and Aims of Geomorphological Mapping. *Developments in Earth Surface Processes*, 15, p.39-73. DOI: 10.1016/B978-0-444-53446-0.00003-3.

Embabi, N.S. and Moawad, M.B., 2014. A semi-automated approach for mapping geomorphology of El Bardawil Lake, Northern Sinai, Egypt, using integrated remote sensing and GIS techniques. *The Egyptian Journal of Remote Sensing and Space Sciences*, 17, p.41-60. DOI: 10.1016/j.ejrs.2014.02.002.

Fan, Z., Zhang, B., Du, Z., Zheng, J., Jun Luo, N.N., Wang, J., and Wang, Q., 2022. Geomorphological regionalization using the Upscaled DEM: the Beijing-Tianjin-Hebei Area, China Case Study. *Nature research-Scientific reports*, 10:10532. DOI: 10.1038/s41598-020-66993-9.

Garcia, G.P.B. and Grohmann, C.H., 2019. DEM-based geomorphological mapping and landforms characterization of a tropical karst environment in southeastern Brazil. *Journal of South American Earth Sciences*, 93, p.14-22 DOI: 10.1016/j.jsames.2019.04.01.

Gregory, K.J. and Walling, D.E., 1973. Drainage basin characteristics: A geographical approach. *Drainage basin form and processes*, Edward Arnold publication, London.

Hack, J.T., 1973. Stream profile analysis and stream gradient index. *Journal of Research of the U. S. Geological Survey*, 1 (4), p.421-429.

Horton, R.E., 1945. Erosional development of streams and their drainage basins: Hydrophysical approach to quantitative morphology. *Geological Society of America Bulletin*, 56, p.275-370.

Imsong, W., Choudhary, S., Phukan, S., and Duarah, B.P., 2018. Morpho-dynamics of Kulsi River Basin in the northern front of Shillong Plateau: Exhibiting episodic inundation and channel migration. *Journal of Earth System Science*, 127 (5), p.1-15. DOI: 10.1007/s12040-017-0904-1.

Lemenkova, P., 2019. Geomorphological modelling and mapping of the Peru-Chile Trench by GMT. *Polish Cartographical Review*, 51 (4), p.181-194. DOI: 10.2478/pcr-2019-0015.

Leopold, L.B. and Maddock, T.J., 1953. The hydraulic geometry of stream channels and some physiographic implications, *Geological Survey Professional Paper,* 252.

Mackin, H.J., 1948. Concept of the graded river; *Geological Society of America,* 55, p.463-512.

Meij, W.M., Meijles, E.W., Marcos, D., Harkema, T.T.L., Candel, J.H.J., and Maas, G.J., 2022. Comparing geomorphological maps made manually and by deep learning. *Earth Surface*

Processes and Landforms, 47, p.1089-1107. DOI: 10.1002/esp.5305.

Napieralski, J., Barr, I., Kamp, U., Kervyn D., and Meerendre, M., 2013. Remote Sensing and GIScience in Geomorphological Mapping. *In:* Schroder J.F, (ed.), *Treatise in Geomorphology*, 3 p.187-227. San Francisco: Academic Press.

NRCS (Natural Resources Conservation Services), 2008. Hydrogeomorphic Wetland Classification System: An Overview and modification to Better Meet the Needs of The Natural Resources Conservation Service. *Technical Note* No. 190-8-76. United States Department of Agriculture.

NMED (New Mexico Environment Department), 2012. New Mexico Wetlands -Wetland Functions, Technical Guide, Surface Water Quality Bureau Wetlands Program, www.env.nm.gov.

Pall, I.A., Meraj, G., and Romshoo, S.A., 2019. Applying integrated remote sensing and field-based approach to map glacial landform features of the Machoi Glacier valley, NW Himalaya. *SN Applied Sciences,* 1, p.488. DOI: 10.1007/s42452-019-0503-7.

Patel, N.K. and Pati, P., 2022. Mapping of the Buried Paleochannels on the Terminal Fans in the Western Ganga Plain: A Geomorphological and Ground Penetrating Radar-based Approach. *Journal of the Geological Society of India*, 98, p.525-537. DOI: 10.1007/s12594-022-2010-5.

Patton, P. and Baker, V., 1976. Morphometry and floods in small Drainage Basin Subject of Diverse Hydrogeomorphic controls, *Water Resource Research*, 12, p.441-952.

Peter, T., 2011. Maps of the imagination: The writer as cartographer. Trinity University Press.

Prodanov, B., Lambev, T., Bekova, R., and Kotsev, I., 2019. Applying Unmanned Aerial Vehicles for High-Resolution Geomorphological Mapping of the Ahtopol Coastal Sector (Bulgarian Black Sea Coast), 219th *International Multidisciplinary Scientific Geo Conference SGEM*, p. 465-472. DOI: 10.5593/sgem2019/2.2.

Rao, D.P., 2002. Remote sensing application in geomorphology. *Tropical Ecology,* 43 (1), p.49-59.

Reddy, G.P.O., 2018. Remote Sensing and GIS for Geomorphological Mapping. *In*: Reddy, G., and Singh, S. (eds.), Geospatial Technologies in Land Resources Mapping, Monitoring and Management. *Geotechnologies and the Environment,* 21, p.223-252. DOI: 10.1007/978-3-319-78711-4_12.

Riley, S.J., 1999. Index that quantifies topographic heterogeneity. *International Journal of Internet Science,* 5, p.23-27.

Shah, R.A. and Lone, S.A., 2019. Hydro-geomorphological mapping using geospatial techniques for assessing the groundwater potential of Rambiara river basin, western Himalayas. *Applied Water Science,* 9 (64). DOI: 10.1007/s13201-019-0941-9.

Smith, M.J., Paron, P., and Griffiths, J.S., 2011. Geomorphological mapping: methods and applications. *Developments in Earth Surface Process*, 15, Elsevier.

Tate, J., 2006. Terrain analysis for decision-making. *In*: Mang, R., and Hausler, H. (eds.), *International Handbook Military Geography*. Ministry of Defense, Vienna, p.321-333.

Teeuw, R.M., 2007. *Mapping Hazardous Terrain Using Remote Sensing*. Geological Society, London, *Special Publication,* 283.

Thomson, E.H. and Sorenson, E.R., 2005. *Wetland, Woodland, and Wildland-A Guide to the natural committee of Vermont.* Vermont Department of Fish and Wildlife and The Nature Conservancy.

Van Asselen, S. and Seijmonsbergen, A.C., 2006. Expert-driven semi-automated geomorphological mapping for a mountainous area using a laser DTM. *Geomorphology,* 78, p.309-320.

Van Lanen, R.J., Kosian, M.C., Groenewoudt, B.J., and Jansma, E., 2015. Finding a way: Modeling landscape prerequisites for Roman and early-medieval routes in the Netherlands. *Geoarchaeology*, 30 (3), p.200-222. DOI: 10.1002/gea.21510.

Whipple, K. and Tucker, G., 2002. Implications of sediment flux dependent river incision models

for landscape evolution. *Journal of Geophysical Research, (Solid Earth),* 107 (B2), p. 2039. DOI: 10.1029/200JB000044.

Whittaker, A.C., Cowie, P.A., Attal, M., Tucker, G.E., and Roberts, G.P., 2007. Bedrock channel adjustment to tectonic forcing: Implications for predicting river incision rates. *Geological Society of America,* 35 (2), p.103-106.

Yin, A., Dubey, C.S., Webb, A.A.G., Kelty, T.K., Grove, M., Gehrels, G.E., and Burges, W. P., 2010. Geologic correlation of the Himalayan orogen and Indian craton: Part I, Structural geology, U-Pb zircon geochronology and tectonic evolution of the Shillong Plateau and its neighboring regions in NE India. *Geological Society of America Bulletin*, 122, p.336-359.

Zhang, B., Fan, Z., Du, Z., Zheng, J., Luo, J., Wang, N., Wang, Q., 2020. A Geomorphological Regionalization using the Upscaled DEM: the Beijing-Tianjin-Hebei Area, China Case Study. *Scientific Reports*, 10, 10532pp. DOI: 10.1038/s41598-020-66993-9

Zinck, J.A., 2013. *GEOPEDOLOGY*: *Elements of geomorphology for soil geohazard studies*. Faculty of Geo-information Science and Earth Observation, Enschede, The Netherland.

IJOG